

Determinations of form factors for semileptonic $D \rightarrow K$ decays and leptoquark constraints

Jian Zhang* Chong-Xing Yue[†]
Chun-Hua Li[‡]

Department of Physics, Liaoning Normal University, Dalian 116029, P. R. China

September 5, 2018

Abstract

By analyzing all existing measurements for $D \rightarrow K\ell^+\nu_\ell$ ($\ell = e, \mu$) decays, we find that the determinations of both the vector form factor $f_+^K(q^2)$ and scalar form factor $f_0^K(q^2)$ for semileptonic $D \rightarrow K$ decays from these measurements are feasible. By taking the parameterization of the one order series expansion of the $f_+^K(q^2)$ and $f_0^K(q^2)$, $f_+^K(0)|V_{cs}|$ is determined to be 0.7182 ± 0.0029 , and the shape parameters of $f_+^K(q^2)$ and $f_0^K(q^2)$ are $r_{+1} = -2.16 \pm 0.007$ and $r_{01} = 0.89 \pm 3.27$, respectively. Combining with the average $f_+^K(0)$ of $N_f = 2 + 1$ and $N_f = 2 + 1 + 1$ lattice calculation, the $|V_{cs}|$ is extracted to be $0.964 \pm 0.004 \pm 0.019$ where the first error is experimental and the second theoretical. Alternatively, the $f_+^K(0)$ is extracted to be $0.7377 \pm 0.003 \pm 0.000$ by taking the $|V_{cs}|$ as the value from the global fit with the unitarity constraint of the CKM matrix. Moreover, using the obtained form factors by $N_f = 2 + 1 + 1$ lattice QCD, we re-analyze these measurements in the context of new physics. Constraints on scalar leptoquarks are obtained for different final states of semileptonic $D \rightarrow K$ decays.

1 Introduction

Semileptonic $D \rightarrow P(P = K, \pi)$ decays have long been of great interest in the field of flavor physics. They play important roles in validating the lattice QCD (LQCD), extracting the Cabibbo-Kobayashi-Maskawa (CKM) matrix elements, and searching for New Physics (NP) beyond the Standard Model (SM) [1].

For the decay $D \rightarrow K\ell^+\nu_\ell$ ($\ell = e, \mu$), strong and weak interaction portions can be well separated and the effects of strong interactions can be parameterized by form factors. In the SM, the differential decay rate as a function of q^2 is given by

$$\frac{d\Gamma(D \rightarrow K\ell^+\nu_\ell)}{dq^2} = \frac{G_F^2 |V_{cs}|^2}{24\pi^3} |\mathbf{p}|^3 \left(1 - \frac{m_\ell^2}{q^2}\right)^2 \cdot \left\{ \left(1 + \frac{m_\ell^2}{2q^2}\right) |f_+^K(q^2)|^2 + \frac{3m_\ell^2(m_D^2 - m_K^2)^2}{8m_D^2 |\mathbf{p}|^2 q^2} |f_0^K(q^2)|^2 \right\}, \quad (1)$$

*E-mail: zhangjianphy@aliyun.com

[†]E-mail: cxyue@lnnu.edu.cn

[‡]E-mail: chunhua@lnnu.edu.cn

where G_F is the Fermi constant, \mathbf{p} represents the three momentum of the K meson in the D rest frame, and $q \equiv p_D - p_K$ is the four momenta transferred to $\ell^+\nu_\ell$ pair. The range of q^2 is from m_ℓ^2 when K has the maximum possible momentum to $(m_D - m_K)^2$ when the K meson is at rest. The vector form factor $f_+^K(q^2)$ and the scalar form factor $f_0^K(q^2)$ are defined via

$$\langle K(p_K) | \bar{s} \gamma^\mu c | D(p_D) \rangle = \left(p_D^\mu + p_K^\mu - \frac{m_D^2 - m_K^2}{q^2} q^\mu \right) f_+^K(q^2) + \frac{m_D^2 - m_K^2}{q^2} q^\mu f_0^K(q^2), \quad (2)$$

and

$$\langle K(p_K) | \bar{s} c | D(p_D) \rangle = \frac{m_D^2 - m_K^2}{m_c - m_s} f_0^K(q^2). \quad (3)$$

At the maximal recoil point, kinematic constraints lead $f_+^K(0) = f_0^K(0)$.

In the last 30 years, various measurements of the decay $D \rightarrow K \ell^+ \nu_\ell$ were performed at more than ten experiments. The decay rates of $D^0 \rightarrow K^- \ell^+ \nu_\ell$ and $D^+ \rightarrow \bar{K}^0 \ell^+ \nu_\ell$ in different q^2 bins were measured at the experiments the E691 [2], E687 [3, 4], E653 [5], Mark-III [6], CLEO [7], FOCUS [8], CLEO-II [9], BaBar [10], BES-II [11–14], CLEO-c [15] and BES-III [16–19]. The FOCUS experiment measured non-parametric relative form factor from $D^0 \rightarrow K^- \mu^+ \nu_\mu$ in 2005 [20], and the Belle experiment measured the vector form factor from $D^0 \rightarrow K^- \ell^+ \nu_\ell$ in 2006 [21]. By combining these measurements, one can obtain $f_+^K(0) |V_{cs}|$, the product of the hadronic form factor at $q^2 = 0$ and the magnitude of CKM matrix element V_{cs} . With the values of $|V_{cs}|$ from the the global fit with the unitarity constraint of CKM matrix and $f_+^K(0)$ calculated in lattice QCD, $f_+^K(0)$ and $|V_{cs}|$ can be extracted from $f_+^K(0) |V_{cs}|$, respectively [22]. In 2014, ref. [22] extract $f_+^K(0)$ and $|V_{cs}|$ by considering all the experimental measurements of $D \rightarrow K e^+ \nu_e$ decays before 2014.

In these experimental and theoretical studies, the contribution of f_0 term is neglected since it is suppressed by the mass squared of lepton. However, with the improvement of experimental precision, it is feasible to determine both the vector and scalar form factors. Here, we determine both $f_+^K(q^2)$ and $f_0^K(q^2)$ for the first time by comprehensively analyzing all the experimental measurements of $D \rightarrow K \ell^+ \nu_\ell$. As the result of this analysis, we report the values of $f_+^K(0) |V_{cs}|$, r_{+1} and r_{01} which are the shape parameters of $f_+^K(q^2)$ and $f_0^K(q^2)$, respectively. We determine $f_+^K(0)$ from $f_+^K(0) |V_{cs}|$ by taking $|V_{cs}|$ as the value obtained from the global fit with the unitarity constraint of CKM matrix done by the Particle Data Group (PDG) in 2016 [23]. $|V_{cs}|$ is extracted with the value of $f_+^K(0)$ calculated in LQCD.

In addition, a comprehensive analysis of these measurements is important to search for non-Standard interactions beyond the Standard weak to $D \rightarrow K \ell^+ \nu_\ell$. One candidate of the non-Standard interactions is to exchange a scalar leptoquark [24–26]. Leptoquarks are hypothetical color-triplet bosons that carry both baryon number and lepton number, and can thus couple directly to a quark and a lepton [27, 28]. Leptoquark can be of either vector (spin-1) or scalar (spin-0) nature according to their properties under the Lorentz transformations. Some scalar leptoquarks can lead to the effective $\bar{s} c \bar{\nu} \ell$ vertex. Searching for the scalar leptoquarks from $D \rightarrow K \ell^+ \nu_\ell$ is one of the goals of this article. By taking the form factors from lattice calculations, we re-analyze the experimental measurements of $D \rightarrow K \ell \nu_\ell$ in the context of new physics and provide the constraint on scalar leptoquark.

The article is organized as follows: We review the parameterization of the form factors in Section 2 firstly, and then present the details of the experimental measurements of $D \rightarrow K \ell^+ \nu_\ell$ in Section 3. The procedure of the analysis is described in Section 4. In Section 5, we study these experimental measurements in the context of new physics. Finally, the conclusions of this work are given in Section 6.

Table 1: Ratios $\mathcal{R}_{0(+)}^\ell$ measured at different experiments.

Experiment	q^2 (GeV)	$\mathcal{R}_{0(+)}^\ell$
E691 [2]	(m_e^2, q_{max}^2)	$\mathcal{R}_0^e = 0.91 \pm 0.07 \pm 0.11$
E687 [3]	(m_μ^2, q_{max}^2)	$\mathcal{R}_0^\mu = 0.82 \pm 0.13 \pm 0.13$
E687 [4]	(m_μ^2, q_{max}^2)	$\mathcal{R}_0^\mu = 0.852 \pm 0.034 \pm 0.028$
CLEO [7]	(m_e^2, q_{max}^2)	$\mathcal{R}_0^e = 0.90 \pm 0.06 \pm 0.06$
CLEO [7]	(m_μ^2, q_{max}^2)	$\mathcal{R}_0^\mu = 0.79 \pm 0.08 \pm 0.09$
CLEO-II [9]	(m_e^2, q_{max}^2)	$\mathcal{R}_0^e = 0.978 \pm 0.027 \pm 0.044$
CLEO-II [9]	(m_e^2, q_{max}^2)	$\mathcal{R}_+^e = 2.60 \pm 0.35 \pm 0.26$
BaBar [10]	(m_e^2, q_{max}^2)	$\mathcal{R}_0^e = 0.927 \pm 0.007 \pm 0.012$

2 Parameterization of the form factors

The form factors $f_+^K(q^2)$ and $f_0^K(q^2)$ can be parameterized according to the constraints of their general properties of analyticity, cross symmetry, and unitarity [29]. Various parameterizations exist such as the single pole model [30], the modified pole model [30], the *ISGW2* model [31] and the *series expansion* [32]. The experimental data, however, does not support the former three models well [22], so the *series expansion* is used in this article. In this parameterization, the form factors transformed from q^2 -space to z -space, where

$$z(q^2, t_0) = \frac{\sqrt{t_+ - q^2} - \sqrt{t_+ - t_0}}{\sqrt{t_+ - q^2} + \sqrt{t_+ - t_0}}, \quad (4)$$

with $t_\pm = (m_D \pm m_K)^2$ and $t_0 = t_+(1 - \sqrt{1 - t_-/t_+})$. The form factors is then expressed as

$$f_{+(0)}^K(q^2) = \frac{1}{\mathcal{P}_{+(0)}(q^2)\phi(q^2, t_0)} \sum_{k=0}^{\infty} a_k^{+(0)}(t_0)[z(q^2, t_0)]^k, \quad (5)$$

where $a_k(t_0)$ are real coefficients. The function $\mathcal{P}_+(q^2)$ is $\mathcal{P}_+(q^2) = z(q^2, m_{D_s^*}^2)$ for $f_+^K(q^2)$ and $\mathcal{P}_0(q^2)$ is $\mathcal{P}_0(q^2) = z(q^2, m_{D_s^0}^2)$ for $f_0^K(q^2)$. $\phi(q^2, t_0)$ is chosen to be

$$\phi(q^2, t_0) = \left(\frac{\pi m_c^2}{3}\right)^{1/2} \left(\frac{z(q^2, 0)}{-q^2}\right)^{5/2} \left(\frac{z(q^2, t_0)}{t_0 - q^2}\right)^{-1/2} \left(\frac{z(q^2, t_-)}{t_- - q^2}\right)^{-3/4} \frac{(t_+ - q^2)}{(t_+ - t_0)^{1/4}}, \quad (6)$$

where m_c is the mass of the charm quark.

By using the relation $1 = f_+^K(0)\mathcal{P}(0)\phi(0, t_0)/(\sum_{k=0}^{\infty} a_k(t_0)[z(0, t_0)]^k)$ deduced from Eq.(5), we obtain

$$f^K(q^2) = \frac{f_+^K(0)\mathcal{P}(0)\phi(0, t_0)(1 + \sum_{k=1}^N r_k[z(q^2, t_0)]^k)}{\mathcal{P}(q^2)\phi(q^2, t_0)(1 + \sum_{k=1}^N r_k[z(0, t_0)]^k)}, \quad (7)$$

where $r_k = a_k(t_0)/a_0(t_0)$ and N is the expansion order.

3 Experimental measurements

The existing measurements for $D^0 \rightarrow K^-\ell^+\nu_\ell$ and $D^+ \rightarrow \bar{K}^0\ell^+\nu_\ell$ can be divided into three categories:

Table 2: Branching fractions $\mathcal{B}_{0(+)}^\ell(D \rightarrow K\ell^+\nu_\ell)$ measured at different experiments.

Experiment	q^2 (GeV)	$\mathcal{B}_{0(+)}^\ell$ (%)
E653 [5]	(m_μ^2, q_{max}^2)	$\mathcal{B}_0^\mu = 3.16 \pm 0.52$
Mark-III [6]	(m_e^2, q_{max}^2)	$\mathcal{B}_0^e = 3.4 \pm 0.5 \pm 0.4$
FOCUS [8]	(m_μ^2, q_{max}^2)	$\mathcal{B}_+^\mu = 9.15 \pm 0.94$
BES-II [11]	(m_e^2, q_{max}^2)	$\mathcal{B}_0^e = 3.82 \pm 0.40 \pm 0.27$
BES-II [12]	(m_e^2, q_{max}^2)	$\mathcal{B}_+^e = 8.95 \pm 1.59 \pm 0.67$
BES-II [13]	(m_μ^2, q_{max}^2)	$\mathcal{B}_0^\mu = 3.55 \pm 0.56 \pm 0.59$
BES-II [14]	(m_μ^2, q_{max}^2)	$\mathcal{B}_+^\mu = 10.3 \pm 2.3 \pm 0.8$
BES-III [17]	(m_e^2, q_{max}^2)	$\mathcal{B}_+^e = 8.59 \pm 0.14 \pm 0.21$
BES-III [18]	(m_μ^2, q_{max}^2)	$\mathcal{B}_+^\mu = 8.72 \pm 0.07 \pm 0.18$

(i) Ratio of the branching fractions $\mathcal{R}_{0(+)}^\ell$, where $\mathcal{R}_0^\ell = \mathcal{B}^\ell(D^0 \rightarrow K^-\ell^+\nu_\ell)/\mathcal{B}(D^0 \rightarrow K^-\pi^+)$, and $\mathcal{R}_+^\ell = \mathcal{B}^\ell(D^+ \rightarrow \bar{K}^0\ell^+\nu_\ell)/\mathcal{B}(D^+ \rightarrow \bar{K}^0\pi^+)$. The ratios measured at different experiments are listed in Table 1.

(ii) Decay branching fraction $\mathcal{B}_{0(+)}^\ell$, where \mathcal{B}_0^ℓ and \mathcal{B}_+^ℓ is the branching fraction of $D^0 \rightarrow K^-\ell^+\nu_\ell$ and $D^+ \rightarrow \bar{K}^0\ell^+\nu_\ell$, respectively. The measurements of $\mathcal{B}_{0(+)}^\ell$ at different experiments are shown in Tab. 2. For the sake of convenience, the ratios $\Gamma(D^0 \rightarrow K^-\mu^+\nu_\mu)/\Gamma(D^0 \rightarrow \mu^+X) = 0.472 \pm 0.051 \pm 0.040$ measured at E653 experiment [5] and $\Gamma(D^+ \rightarrow \bar{K}^0\mu^+\nu_\mu)/\Gamma(D^+ \rightarrow K^-\pi^+\pi^+) = 1.019 \pm 0.076 \pm 0.065$ measured at the FOCUS experiment [8] have been transformed into corresponding branching fractions also listed in Tab. 2 by using $B(D^0 \rightarrow \mu^+X) = (6.7 \pm 0.6)\%$ and $B(D^+ \rightarrow K^-\pi^+\pi^+) = (8.98 \pm 0.28)\%$ which are taken from PDG [33].

(iii) Decay rate $\Delta\Gamma$, where $\Delta\Gamma$ represents the partial decay rate of $D^0 \rightarrow K^-e^+\nu_e$ or $D^+ \rightarrow \bar{K}^0e^+\nu_e$ in a certain q^2 bin.

Measurements of the first two categories could not be used directly to determine $f_+^K(0)|V_{cs}|$ and the shapes of form factors. To use these measurements, we should first transfer them into absolute decay rates in certain q^2 ranges [22].

The absolute decay rates for the experimental results classified as the categories (i) and (ii) measurements can be extracted respectively by

$$\Delta\Gamma = \mathcal{R} \times \mathcal{B}(D \rightarrow K\pi) \times \frac{1}{\tau_D}, \quad (8)$$

and

$$\Delta\Gamma = \mathcal{B}(D \rightarrow K\ell^+\nu_\ell) \times \frac{1}{\tau_D}, \quad (9)$$

where $\mathcal{B}(D \rightarrow K\pi)$ is the branching fraction for $D^0 \rightarrow K^-\pi^+$ or $D^+ \rightarrow \bar{K}^0\pi^+$ decays, and τ_D is the lifetime of D^0 or D^+ meson. To avoid the possible correlations, we use $\mathcal{B}(D^0 \rightarrow K^-\pi) = (3.89 \pm 0.04)\%$, $\mathcal{B}(D^+ \rightarrow \bar{K}^-\pi^+) = (2.93 \pm 0.094)\%$ which is the sum of $\mathcal{B}(D^+ \rightarrow K_S^0\pi^+) = (1.47 \pm 0.08)\%$ and $\mathcal{B}(D^+ \rightarrow K_L^0\pi^+) = (1.46 \pm 0.05)\%$, $\tau_{D^0} = (410.1 \pm 1.5) \times 10^{-15}$ s, $\tau_{D^+} = (1040 \pm 7) \times 10^{-15}$ s from PDG [33].

The absolute decay rates after the transformations and the measurements, classified as the category (iii), of partial decay rates in different q^2 bins for $D \rightarrow Ke^+\nu_e$, are shown in Tabs. 3 and 4.

We also consider the non-parametric relative form factors $f_+^K(q^2)$ for $D^0 \rightarrow K^-\mu^+\nu_\mu$ measured at the FOCUS experiment in 2005 [20]. The average values of relative form factors $f_+^K(q^2)$ in nine q^2 bins

Table 3: Partial decay rates $\Delta\Gamma$ of $D^0 \rightarrow K^- \ell^+ \nu_\ell$ decays in q^2 ranges.

Experiment	q^2 (GeV)	$\Delta\Gamma$ (ns ⁻¹)
E691 [2]	(m_e^2, q_{max}^2)	86.32 ± 12.40
CLEO [7]	(m_e^2, q_{max}^2)	85.37 ± 8.10
CLEO-II [9]	(m_e^2, q_{max}^2)	92.77 ± 5.00
BaBar [10]	(m_e^2, q_{max}^2)	87.92 ± 1.63
E687 [3]	(m_μ^2, q_{max}^2)	77.78 ± 17.46
E687 [4]	(m_μ^2, q_{max}^2)	80.82 ± 4.27
CLEO [7]	(m_μ^2, q_{max}^2)	74.94 ± 11.45
Mark-III [6]	(m_e^2, q_{max}^2)	82.91 ± 15.62
BES-II [11]	(m_e^2, q_{max}^2)	93.15 ± 11.77
E653 [5]	(m_μ^2, q_{max}^2)	77.11 ± 12.65
BES-II [13]	(m_μ^2, q_{max}^2)	86.56 ± 19.84
CLEO-c [15]	$(m_e^2, 0.2)$	17.82 ± 0.43
	$(0.2, 0.4)$	15.83 ± 0.39
	$(0.4, 0.6)$	13.91 ± 0.36
	$(0.6, 0.8)$	11.69 ± 0.32
	$(0.8, 1.0)$	9.36 ± 0.28
	$(1.0, 1.2)$	7.08 ± 0.24
	$(1.2, 1.4)$	5.34 ± 0.21
	$(1.4, 1.6)$	3.09 ± 0.16
	$(1.6, q_{max}^2)$	1.28 ± 0.11
BES-III [16]	$(m_e^2, 0.1)$	8.812 ± 0.187
	$(0.1, 0.2)$	8.743 ± 0.162
	$(0.2, 0.3)$	8.295 ± 0.159
	$(0.3, 0.4)$	7.567 ± 0.153
	$(0.4, 0.5)$	7.486 ± 0.152
	$(0.5, 0.6)$	6.446 ± 0.138
	$(0.6, 0.7)$	6.200 ± 0.134
	$(0.7, 0.8)$	5.519 ± 0.126
	$(0.8, 0.9)$	5.028 ± 0.119
	$(0.9, 1.0)$	4.525 ± 0.111
	$(1.0, 1.1)$	3.972 ± 0.103
	$(1.1, 1.2)$	3.326 ± 0.093
	$(1.2, 1.3)$	2.828 ± 0.085
	$(1.3, 1.4)$	2.288 ± 0.077
	$(1.4, 1.5)$	1.737 ± 0.068
	$(1.5, 1.6)$	1.314 ± 0.058
	$(1.6, 1.7)$	0.858 ± 0.050
$(1.7, q_{max}^2)$	0.379 ± 0.039	

Table 4: Partial decay rates $\Delta\Gamma$ of $D^+ \rightarrow \bar{K}^- \ell^+ \nu_\ell$ decays in q^2 ranges.

Experiment	q^2 (GeV ²)	$\Delta\Gamma$ (ns ⁻¹)
CLEO-II [9]	(m_e^2, q_{max}^2)	73.25 ± 12.52
BES-II [12]	(m_e^2, q_{max}^2)	86.06 ± 16.60
BES-III [17]	(m_e^2, q_{max}^2)	82.60 ± 2.49
FOCUS [8]	(m_μ^2, q_{max}^2)	87.99 ± 9.08
BES-II [14]	(m_μ^2, q_{max}^2)	99.04 ± 23.42
BES-III [18]	(m_μ^2, q_{max}^2)	83.85 ± 1.94
CLEO-c [15]	$(m_e^2, 0.2)$	17.79 ± 0.65
	$(0.2, 0.4)$	15.62 ± 0.59
	$(0.4, 0.6)$	14.02 ± 0.54
	$(0.6, 0.8)$	12.28 ± 0.49
	$(0.8, 1.0)$	8.92 ± 0.41
	$(1.0, 1.2)$	8.17 ± 0.37
	$(1.2, 1.4)$	4.96 ± 0.27
	$(1.4, 1.6)$	2.67 ± 0.19
	$(1.6, q_{max}^2)$	1.19 ± 0.13
BES-III [19]	$(m_e^2, 0.2)$	16.97 ± 0.60
	$(0.2, 0.4)$	15.29 ± 0.53
	$(0.4, 0.6)$	13.57 ± 0.47
	$(0.6, 0.8)$	11.65 ± 0.40
	$(0.8, 1.0)$	9.33 ± 0.34
	$(1.0, 1.2)$	7.06 ± 0.28
	$(1.2, 1.4)$	4.96 ± 0.20
	$(1.4, 1.6)$	2.97 ± 0.14
		$(1.6, q_{max}^2)$

Table 5: Non-parametric relative form factors $f_+^K(q_i^2)$ measured at the FOCUS experiment.

i	q^2 (GeV)	$f_+^K(q^2)$
1	0.09	1.01 ± 0.03
2	0.27	1.11 ± 0.05
3	0.45	1.15 ± 0.07
4	0.63	1.17 ± 0.08
5	0.81	1.24 ± 0.09
6	0.99	1.45 ± 0.09
7	1.17	1.47 ± 0.11
8	1.35	1.48 ± 0.16
9	1.53	1.84 ± 0.19

were obtained by assuming $f_+^K(0)$ has been normalized to 1 and the ratio $f_-^K(q^2)/f_+^K(q^2) = -0.7$, where $f_-^K(q^2) = (f_0^K(q^2) - f_+^K(q^2))(m_D^2 - m_K^2)/q^2$. The measurements are listed in Tab. 5.

In 2006, the Belle collaboration reported the measurements of $f_+^K(q^2)$ for $D^0 \rightarrow K^- \ell^+ \nu_\ell$ decays [21]. Based on the accumulated $56461 \pm 309 \pm 830$ inclusive D^0 mesons, they found $1318 \pm 37 \pm 7$ signal events for the electron mode and $1249 \pm 37 \pm 25$ signal events for the muon mode. In neglecting the lepton masses, they obtained $f_+^K(q^2)$ in 27 q^2 bins with the bin size of 0.067 GeV^2 . It is worthy to note that these measurements were obtained in the case of the masses of ignoring leptons, so the vector form factor is different from the one defined in this article. To make a distinction between these vector form factors, we use $f_+^{NL}(q^2)$ to represent the vector form factor in the case of neglecting the mass of lepton. In order to use these measurements in this work, we translate them into products $f_+^{NL}(q_i^2)|V_{cs}|$ by using $|V_{cs}| = 0.97296 \pm 0.00024$, which was used by the Belle experiment to obtain the $f_+^{NL}(q_i^2)$ in their article. The measurements $f_+^{NL}(q_i^2)$ and $f_+^{NL}(q_i^2)|V_{cs}|$ are listed in Tab. 6.

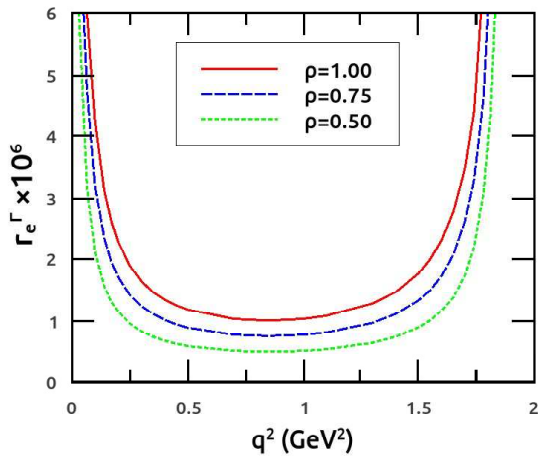
$f_+^K(q^2)$ measured at the FOCUS experiment and $f_+^{NL}(q^2)|V_{cs}|$ measured at the Belle experiment are important for the determination of $f_0^K(q^2)$ for semileptonic $D \rightarrow K$ decays. We will discuss this issue in the next section.

4 Fits to experimental data in the context of the SM

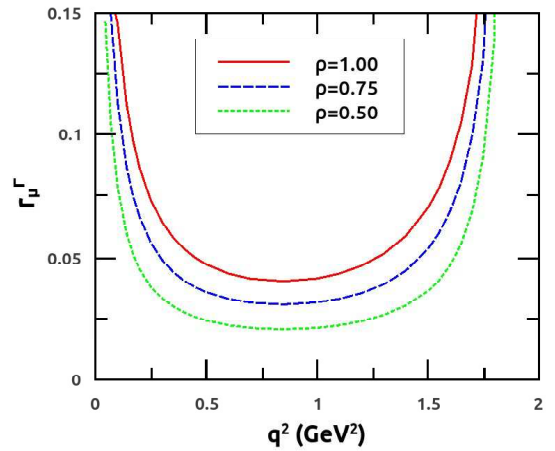
Our goal is to obtain the product $f_+^K(0)|V_{cs}|$ and the shapes of the vector and scalar form factors with semileptonic $D \rightarrow K$ decays from the existing experimental measurements. Firstly, we validate the analysis scheme by analyzing these experimental data, which is depending on the relative errors of these measurements and the contribution ratios of f_0^K term to these measurements. If the contributions of f_0^K to these measurements are much smaller than the errors of these measurements, the fitting result of the scalar form factor will not be credible, so the confirmation of the feasibility is very important.

Table 6: $f_+^{NL}(q_i^2)$ and $f_+^{NL}(q_i^2)|V_{cs}|$ measured at the Belle experiment.

i	q^2 (GeV)	$f_+^{NL}(q_i^2)$	$f_+^{NL}(q_i^2) V_{cs} $
1	0.100	0.711 ± 0.034	0.692 ± 0.033
2	0.167	0.787 ± 0.034	0.766 ± 0.033
3	0.233	0.764 ± 0.034	0.743 ± 0.033
4	0.300	0.838 ± 0.034	0.815 ± 0.033
5	0.367	0.788 ± 0.037	0.767 ± 0.036
6	0.433	0.843 ± 0.039	0.820 ± 0.038
7	0.500	0.882 ± 0.043	0.858 ± 0.042
8	0.567	0.942 ± 0.045	0.917 ± 0.044
9	0.633	0.910 ± 0.045	0.885 ± 0.044
10	0.700	0.823 ± 0.045	0.801 ± 0.044
11	0.767	1.028 ± 0.048	1.000 ± 0.047
12	0.833	1.000 ± 0.049	0.973 ± 0.048
13	0.900	0.949 ± 0.050	0.923 ± 0.049
14	0.967	1.046 ± 0.057	1.018 ± 0.055
15	1.033	1.100 ± 0.057	1.070 ± 0.055
16	1.100	0.941 ± 0.062	0.916 ± 0.060
17	1.167	1.114 ± 0.069	1.084 ± 0.067
18	1.233	1.100 ± 0.075	1.070 ± 0.073
19	1.300	1.249 ± 0.086	1.215 ± 0.084
20	1.367	1.381 ± 0.093	1.344 ± 0.090
21	1.433	1.313 ± 0.107	1.278 ± 0.104
22	1.500	1.190 ± 0.112	1.158 ± 0.109
23	1.567	1.416 ± 0.127	1.378 ± 0.124
24	1.633	1.471 ± 0.175	1.431 ± 0.170
25	1.700	1.417 ± 0.222	1.379 ± 0.216
26	1.767	1.150 ± 0.345	1.120 ± 0.336
27	1.833	1.450 ± 0.915	1.411 ± 0.890



(a)



(b)

Figure 1: The contributions of f_0 term to the differential decay rates for $D \rightarrow Ke^+\nu_e$ decays (a) and $D \rightarrow K\mu^+\nu_\mu$ decay (b).

4.1 The contribution of scalar form factor

The contribution of f_0 term to the differential decay rate of $D \rightarrow K\ell^+\nu_\ell$ at a certain q^2 can be described by the ratio

$$\begin{aligned} r_\ell^\Gamma(q^2) &= \frac{d\Gamma_\ell^S/dq^2}{d\Gamma(D \rightarrow K\ell\nu_\ell)/dq^2} \\ &= \frac{\rho \frac{3m_\ell^2(m_D^2 - m_K^2)^2}{8m_D^2|\mathbf{p}|^2q^2}}{1 + \frac{m_\ell^2}{2q^2} + \rho \frac{3m_\ell^2(m_D^2 - m_K^2)^2}{8m_D^2|\mathbf{p}|^2q^2}}, \end{aligned} \quad (10)$$

where ρ represents $|f_0^K(q^2)/f_+^K(q^2)|^2$.

$r_e^\Gamma(q^2)$ and $r_\mu^\Gamma(q^2)$ varying with q^2 were shown in Figs. 1 (a) and (b), respectively. The ρ in Eq. 10 is set to $\rho = 1.0, 0.75$ or 0.5 according to previous lattice calculations. Fig. 1 (a) shows that the contribution of f_0^K term to the partial decay rate for $D \rightarrow Ke^+\nu_e$ decay is less than 10^{-5} in the most range of q^2 , which is much smaller than the relative errors of corresponding partial decay rate measured at the experiments listed in Tabs. 3 and 4, so neglecting the contribution of the scalar form factor is a good approximation in analysis for the electron channel. While for the muon channel, Fig. 1 (b) shows that the contribution of f_0^K term to the partial decay rate is $3\% \sim 5\%$ in the most q^2 range which need to be considered when the experimental measurements have high precision. So the extraction of $f_0^K(q^2)$ is feasible especially from the muon channel.

4.2 Construct Chi-squared function

To obtain $f_+^K(0)|V_{cs}|$ and shapes of the vector and scalar form factors, we perform our fit to these experimental measurements by minimizing the Chi-squared function

$$\chi^2 = \chi_{\Delta\Gamma}^2 + \chi_{FOC}^2 + \chi_{Bel}^2, \quad (11)$$

where $\chi_{\Delta\Gamma}^2$ is constructed for measurements of partial decay rates in different q^2 ranges for $D \rightarrow Ke^+\nu_e$ as shown in Tabs. 3 and 4, χ_{FOC}^2 is for the non-parametric form factors $f_+^K(q^2)$ measured at the FOCUS experiment, and χ_{Bel}^2 corresponds to the Belle Collaboration measured products $f_+^{NL}(q_i^2)|V_{cs}|$.

Since there are correlations between the measurements of partial decay rates for $D^0 \rightarrow K^-e^+\nu_e$ decays and/or $D^+ \rightarrow \bar{K}^0e^+\nu_e$ decays, the $\chi_{\Delta\Gamma}^2$ is given by

$$\chi_{\Delta\Gamma}^2 = \sum_{i=1}^{62} \sum_{j=1}^{62} (\Delta\Gamma_i - \Delta\Gamma_i^{th})(C_{\Delta\Gamma}^{-1})_{ij}(\Delta\Gamma_j - \Delta\Gamma_j^{th}), \quad (12)$$

where $\Delta\Gamma$ is the partial decay rate measured in experiment, $\Delta\Gamma^{th}$ denotes its theoretical expectation, and $C_{\Delta\Gamma}^{-1}$ is the inverse of the covariance matrix $C_{\Delta\Gamma}$, which is a 62×62 matrix. To compute the covariances of these 62 partial decay rates measured in different q^2 ranges and at different experiments, we adopt the concept proposed in Ref. [22]: (a) at the same experiment, the statistical and systematic errors of these partial decay rates, and corresponding correlations between these partial decay rates are used to compute their covariances; (b) the systematic uncertainties caused by the lifetime of $D^{0(+)}$ meson are fully correlated among all of the partial decay rates for $D^{0(+)} \rightarrow K^-(\bar{K}^0)e^+\nu_e$ decays measured at different experiments. (c) the systematic uncertainties related to $D^0 \rightarrow K^-\pi^+$ are full correlated among all of the measurements of category (i) in Section 3 for $D^0 \rightarrow K^-e^+\nu_e$ decays.

Due to the correlations between measurements of the non-parametric form factors at the FOCUS experiment, the χ_{FOC}^2 in Eq. 11 is defined as

$$\chi_{FOC}^2 = \sum_{i=1}^9 \sum_{j=1}^9 (\mathbf{f}_i - \mathbf{f}_i^{th})(C_{FOC}^{-1})_{ij}(\mathbf{f}_j - \mathbf{f}_j^{th}), \quad (13)$$

where \mathbf{f}_i and \mathbf{f}_i^{th} are the measured value from the FOCUS experiment and the theoretical expectation of the average of $\mathbf{f}_+^K(q^2)$ over the width of i -th q^2 bin, respectively. It is worth noting that vector form factor $f_+^K(q^2)$ in Eq. 7 can not be used as the theoretical form factor \mathbf{f}_i^{th} directly, because some assumptions about the expression of differential decay rate for $D^0 \rightarrow K^- \mu^+ \nu_\mu$ process are different between this article and Ref. [20]. By comparing Eq. (1) in this article and Eq. (2) in Ref. [20], we can obtain

$$\mathbf{f}_i^{th} = \frac{\left[\int_{q_{i\min}^2}^{q_{i\max}^2} \frac{V_\mu(q^2)|f_+^K(q^2)|^2 + S_\mu(q^2)|f_0^K(q^2)|^2}{V_\mu(q^2) + S_\mu(q^2)(1 + \beta q^2/\alpha)^2} dq^2 \right]^{\frac{1}{2}}}{f_+^K(0)\sqrt{q_{i\max}^2 - q_{i\min}^2}}, \quad (14)$$

where $S_\mu(q^2) = 3m_\mu^2(m_D^2 - m_K^2)^2/(8m_D^2|\mathbf{p}|^2q^2)$, $V_\mu(q^2) = (1 + m_\mu^2/(2q^2))$, $\alpha = (m_D^2 - m_K^2)^2$ and $\beta = f_-^K(q^2)/f_+^K(q^2) = -0.7$. The C_{FOC}^{-1} in Eq. (13) is the inverse of the covariance matrix C_{FOC} , which is a 9×9 matrix. We can construct the covariance matrix C_{FOC} by the relation $(C_{FOC})_{ij} = \sigma_i \sigma_j \rho_{ij}$, where σ_i (σ_j) is the standard error of $\mathbf{f}_+^K(q^2)$ at the central value of the i -th (j -th) q^2 bin measured at the FOCUS experiment, and ρ_{ij} is the correlation coefficient of measurements of $\mathbf{f}_+^K(q^2)$ at i -th q^2 bin and j -th q^2 bin.

The χ_{Bel}^2 in Eq. (11) is built for the products $f_+^{NL}(q_i^2)|V_{cs}|$ measured at the Belle experiment. The χ_{Bel}^2 is defined as

$$\chi_{Bel}^2 = \sum_{i=1}^{27} \left(\frac{F_i - F_i^{th}}{\sigma_i} \right)^2, \quad (15)$$

where F_i and F_i^{th} are experimental and theoretical values of $f_+^{NL}(q_i^2)|V_{cs}|$ in the i -th q^2 bin respectively, and σ_i represents the standard deviation of F_i . In Eq. 15, we neglect some possible correlations among the measurements of $f_+^{NL}(q_i^2)|V_{cs}|$. Similar to the analysis of the measurements at the FOCUS experiment above, by comparing Eq. (1) in this article and Eq. (1) in Ref. [21], the expression of $f_+^{NL}(q_i^2)|V_{cs}|$ is

$$F_i^{th} = \left[\frac{\int_{q_{i\min}^2}^{q_{i\max}^2} \left(0.54 \frac{d\Gamma_e}{dq^2} + 0.46 \frac{d\Gamma_\mu}{dq^2} \right) dq^2}{q_{i\max}^2 - q_{i\min}^2} \frac{24\pi^3}{G_F^2 |\mathbf{p}|^3} \right]^{1/2}, \quad (16)$$

where $d\Gamma_e/dq^2$ and $d\Gamma_\mu/dq^2$ are respectively the Eq. (1) for $D \rightarrow Ke^+\nu_e$ and $D \rightarrow K\mu^+\nu_\mu$ decays. The weights 0.54 and 0.46 are obtained from the branching fractions of $D^0 \rightarrow K^-e^+\nu_e$ and $D^0 \rightarrow K^- \mu^+ \nu_\mu$ and their errors which are in the Belle's paper published. In Eq.(16),

$$|\mathbf{p}|^3 = \frac{\int_{q_{i\min}^2}^{q_{i\max}^2} |\mathbf{p}|^3 |f_+^K(q^2)|^2 dq^2}{|f_+^K(q_i^2)|^2 (q_{i\max}^2 - q_{i\min}^2)}, \quad (17)$$

where $f_+^K(q^2)$ is computed using the simple pole model with $m_{pole} = 1.82 \pm 0.04 \pm 0.03$ GeV which was originally used to obtain $f_+^K(q^2)$ in the Belle's paper published.

Table 7: The extracted values of the parameters $f_+^K(0)|V_{cs}|$, r_{+1} , r_{+2} and r_{01} and the correlation coefficients between them ρ_{ij} in the fittings where i and j with the values from 1 to 4 correspond to the four parameters. r_{+1} and r_{+2} are the shape parameters of $f_+(q^2)$, and r_{01} is of $f_0(q^2)$. The N_V and N_S are the expansion orders of the vector and scalar form factors, respectively. The goodness of fit $\chi^2/\text{d.o.f.}$ is also listed. ”-” means unavailable.

	This work			HFLAV’16	Y. Fang
	(a) $N_V = 1$ $N_S = 1$ $m_\ell \neq 0$	(b) $N_V = 2$ $m_\ell = 0$	(c) $N_V = 2$ $N_S = 1$ $m_\ell \neq 0$	$N_V = 2$ $m_\ell = 0$	$N_V = 2$ $m_\ell = 0$
$f_+^K(0) V_{cs} $	0.7182(29)	0.7169(29)	0.7182(34)	0.7226(32)	0.717(4)
r_{+1}	-2.16(7)	-2.13(11)	-2.16(11)	-2.38(13)	-2.34(17)
r_{+2}	–	-0.84(2.20)	-0.07(2.72)	-4.7(3.0)	0.43(3.82)
r_{01}	0.89(3.27)	–	0.84(3.73)	–	–
Correlations	$\rho_{12}/\rho_{14}/\rho_{24}$ 0.52/-0.32/-0.71	$\rho_{12}/\rho_{13}/\rho_{23}$ -0.007/0.22/-0.87	$\rho_{12}/\rho_{13}/\rho_{14}/$ $\rho_{23}/\rho_{24}/\rho_{34}$ -0.02/0.39/-0.39/ -0.79/0.10/-0.37	$\rho_{12}/\rho_{13}/\rho_{23}$ -0.19/0.51/-0.84	–
$\chi^2/\text{d.o.f.}$	92.334/95	99.2/95	92.331/94	–	100.1/69

4.3 Fit to experimental data

We fit the experimental data with the Eq.1 where the vector and scalar form factors are parameterized as Eq. (7). The contribution of $f_0^K(q^2)$, as shown in Sec.4.1, is relatively small (3% \sim 5%) for the muon case and negligible ($\sim 10^{-4}\%$) for electron due to their small mass, so the extraction of $f_0^K(q^2)$ is sensitive to the parameterization of $f_+^K(q^2)$. The fittings by expanding $f_+^K(q^2)$ to different orders and neglecting the mass of lepton or not are performed. The three fitting schemes are applied, (a) $N_V = 1$, $N_S = 1$ and $m_\ell \neq 0$; (b) $N_V = 2$ and $m_\ell = 0$; (c) $N_V = 2$, $N_S = 1$ and $m_\ell \neq 0$. N_V and N_S are the expansion orders of $f_+^K(q^2)$ and $f_0^K(q^2)$ in Eq. (7), respectively. All of the SM input parameters such as the Fermi constant G_F , the masses of mesons and charged leptons are taken from PDG [33].

The fitting results are listed in the Tab. 7. As a comparison, the results obtained by Heavy Flavor Averaging Group (HFLAV) [34] in 2016 (HFLAV’16) and Y. Fang et al [22] are also listed. The experimental data applied by HFLAV’16, Y. Fang and our work are a bit different. Comparing to the work of HFLAV’16 and Y. Fang, the latest results of the $D^+ \rightarrow \bar{K}^0 e^+ \nu_e$ from BESIII [17, 19] is included in our analysis. In addition, in order to extract $f_0^K(q^2)$ effectively, more measurements for muon channel are added in our work e.g. the total decay rates of $D \rightarrow K \mu^+ \nu_\mu$ measured by E686 [3, 4], E653 [5], CLEO [7], FOCUS [8], BES-II [13, 14], BES-III [18]. The measurement from CLEO-c Ref. [35] is used in HFLAV’16 only.

The parameter setting in the fittings of HFLAV’16 and Y. Fang is to expand $f_+^K(q^2)$ with two orders and neglect the lepton mass, which is the same as the fitting scheme (b) in our work. From the Tab. 7 we can see that the $f_+^K(0)|V_{cs}|$ obtained by HFLAV’16, Fang and our work (b) are consistent within error. The values of the shape parameter r_{+1} and r_{+2} are also consistent within two times of the errors, while r_{+2} has quite large errors. Comparing the results of the schemes (a), (b) and (c) of our work in Tab. 7 we can see that the fitting results have little change with the different

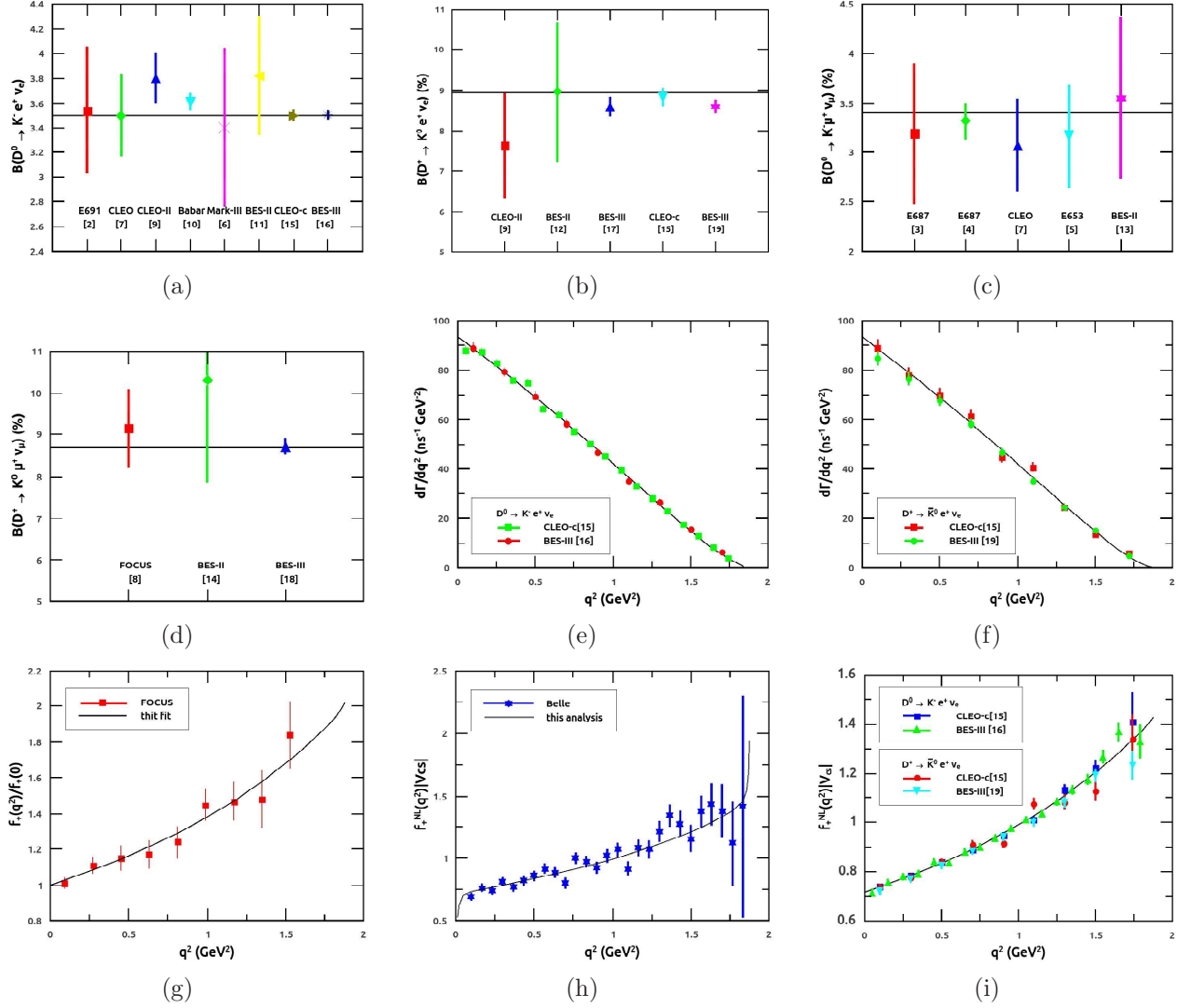


Figure 2: Fit to the experimental measurements. The black lines are the fitting results, and the different symbols are the measurements from different experiments. The branching fractions for $D^0 \rightarrow K^- e^+ \nu_e$ (a), $D^+ \rightarrow \bar{K}^0 e^+ \nu_e$ (b), $D^0 \rightarrow K^- \mu^+ \nu_\mu$ (c) and $D^+ \rightarrow \bar{K}^0 \mu^+ \nu_\mu$ (d) at different experiments. Differential decay rates measured at the CLEO-c and BES-III experiments for $D^0 \rightarrow K^- e^+ \nu_e$ (e) and $D^+ \rightarrow \bar{K}^0 e^+ \nu_e$ (f). The relative form factor $f_+^K(q^2)$ measured at the FOCUS experiment for $D^0 \rightarrow K^- \mu^+ \nu_\mu$ decay (g). The product $f_+^{NL}(q^2)|V_{cs}|$ measured at the Belle experiment for $D^0 \rightarrow K^- \ell^+ \nu_\ell$ ($\ell = e, \mu$) decay (h). The product $f_+^{NL}(q^2)|V_{cs}|$ measured at the CLEO-c and the BES-III experiments for $D \rightarrow K e^+ \nu_e$ decay (i).

settings of the $f_+^K(q^2)$ expansion and the lepton mass. While the $\chi^2/\text{d.o.f.}$ become slightly better when the lepton mass is not neglected. The fit of the scheme (a) is taken as the nominal one, and the corresponding fitting results are shown in the Fig. 2.

4.4 Determinations of $f_+^K(0)$ and $|V_{cs}|$

Note that the fit to experimental data returns just the product of the hadronic form factor $f_+^K(0)$ and the magnitude of CKM matrix element V_{cs} . To determine $f_+^K(0)$ or extract $|V_{cs}|$, we need more inputs. $|V_{cs}|$ can be most precisely determined using a global fit to all available measurements and take three generation unitarity as the SM constrain. The theory predictions for hadronic matrix

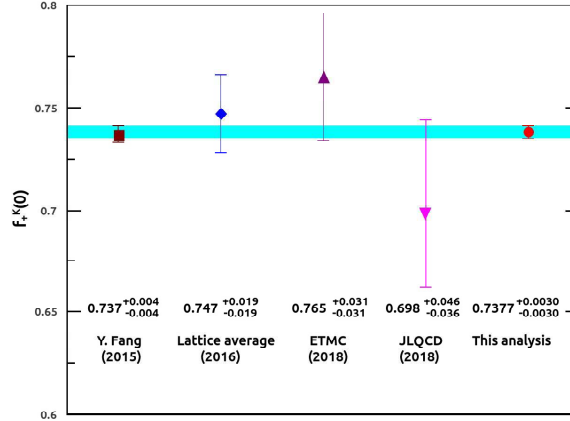


Figure 3: The $f_+^K(0)$ determined with experimental data or Lattice QCD. The values are described in the text. The cyan band is the uncertainty at one standard deviation of this analysis.

elements is also needed in the fit. There are several approaches to combining the experimental data. By considering the product $f_+^K(0)|V_{cs}| = 0.7182 \pm 0.0029$ as shown in Tab. 7 together with $|V_{cs}| = 0.97351 \pm 0.00013$ obtained from the unitarity constraints [33], one can obtain

$$f_+^K(0) = 0.7377 \pm 0.0030 \pm 0.000, \quad (18)$$

where the first error is from the uncertainties in the partial decay rate measurements, and the second is the contribution of the uncertainty of $|V_{cs}|$. The form factor $f_+^K(0)$ determined from recent lattice calculations by the JLQCD collaboration [36] and the ETMC collaboration [37], the average of $N_f = 2 + 1$ lattice calculations before 2017 [38] and experimental fit in 2014 [22] are compared in Fig. 3. Our fitting result is consistent with these theoretical calculations and presents a good consistency with the previous fitting result, but is with higher precision. $f_+^K(0)$ also can be determined from such as light-cone sum rules [39] and the light front quark model [40].

The $f_+^K(q^2)$ and $f_0^K(q^2)$ for semileptonic $D \rightarrow K$ decays are determined and shown in Fig. 4. The recent lattice calculation from JLQCD collaboration with $N_f = 2 + 1$ flavors of dynamical quarks [36] and ETMC collaboration [37] with $N_f = 2 + 1 + 1$ are shown in the plot as well. We can see that the $f_+^K(q^2)$ and $f_0^K(q^2)$ obtained by this work agree well with the JLQCD result within error, and also the ETMC result at low values of q^2 . There are some discrepancies at high values of q^2 between the ETMC and the other two results which is caused by the subtraction of hypercubic artifacts in the ETMC calculation. The hypercubic effects will impact the form factors especially at the high values of q^2 [37]. The precision of the $f_0^K(q^2)$ obtained in the work is low due to the small contribution of the scalar form factor to the decay width as discussed in Section 4.1, which is expected to be improved according to more measurements of the $D \rightarrow K\mu\nu_\mu$ decay.

On the other hand, a comprehensive consideration of $f_+^K(0)|V_{cs}| = 0.7182 \pm 0.0029$ and $f_+^K(0) = 0.745 \pm 0.015$ (the average of lattice calculations $f_+^K(0) = 0.698 \pm 0.041$ obtained by JLQCD collaboration [36], $f_+^K(0) = 0.765 \pm 0.031$ obtained by ETMC [37] and $f_+^K(0) = 0.747 \pm 0.019$ which is the lattice average before 2017 [38]), the magnitude of the CKM matrix element V_{cs} is determined to be

$$|V_{cs}| = 0.964 \pm 0.004 \pm 0.019, \quad (19)$$

where the first error is experimental and the second is theoretical. With comprehensive consideration of the $|V_{cs}| = 0.964 \pm 0.004 \pm 0.019$ extracted in this analysis together with the $|V_{cs}| = 1.008 \pm 0.021$

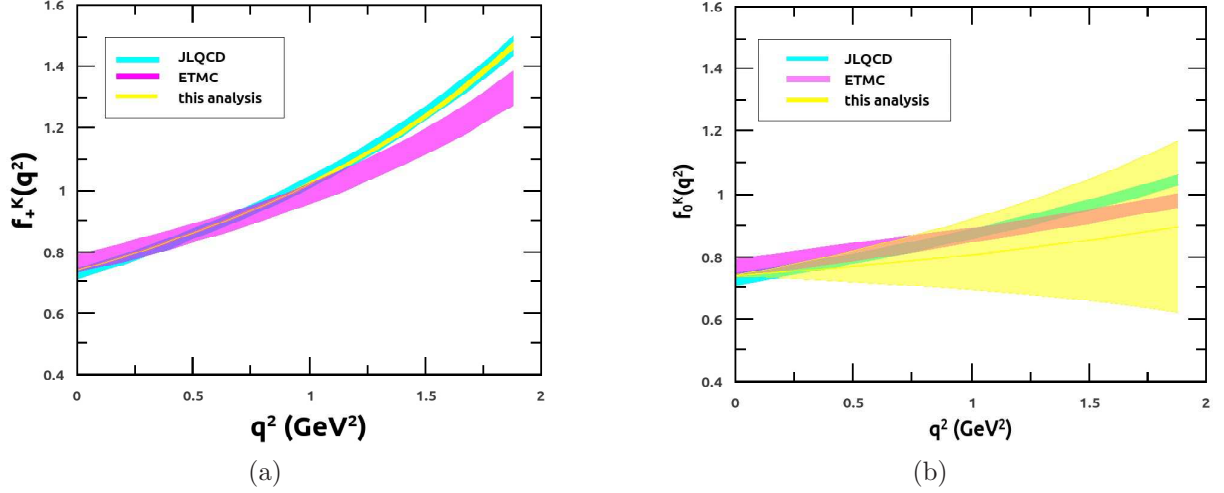


Figure 4: The shapes of $f_+^K(q^2)$ (a) and $f_0^K(q^2)$ (b). The yellow bands are the results of this work. The cyan and pink bands are from the JLQCD [36] and ETMC [37].

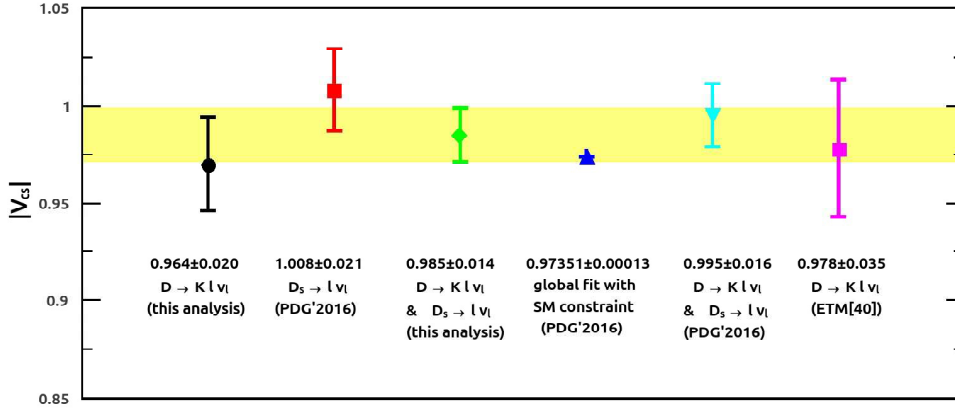


Figure 5: The $|V_{cs}|$ extracted from different analysis. The yellow band is one standard deviation of the green square

determined from leptonic D_s decay [33], the magnitude of the CKM matrix element V_{cs} is determined to be

$$|V_{cs}| = 0.985 \pm 0.014, \quad (20)$$

which is consistent with the average value $|V_{cs}| = 0.995 \pm 0.016$ from PDG'2016 [33]. The ETM collaboration obtained $|V_{cs}| = 0.978 \pm 0.035$ by combining $f_+^K(q^2)$ obtained by their lattice QCD simulations with the differential rates measured for the semileptonic $D \rightarrow K\ell\nu_\ell$ decays [41]. Comparisons of $|V_{cs}|$ extracted from different analysis are shown in Fig. 5.

5 Leptoquark constraints from $D \rightarrow K\ell^+\nu_\ell$ decays

If there exist new interactions beyond the Standard W^+ mediating $c\bar{s} \rightarrow \nu\bar{\ell}$, then they alter the decay rate and q^2 -distribution of $D \rightarrow K\ell\nu_\ell$ decay processes. Since experimental data for $D \rightarrow K\ell\nu_\ell$ decays, at some level, are in good agreement with the SM, the contributions of the new particles should be small and thus these new particles must be too heavy to directly detect. So an effective

Lagrangian extended the SM is considered here. Omitting right-handed neutrinos, the effective Lagrangian is given by [24]

$$\begin{aligned}
\mathcal{L}_{eff} = & - (\sqrt{2}G_F V_{cs}^* + G_V)(\bar{s}\gamma^\mu c)(\bar{\nu}_L\gamma_\mu l_L) \\
& + (\sqrt{2}G_F V_{cs}^* + G_A)(\bar{s}\gamma^\mu\gamma_5 c)(\bar{\nu}_L\gamma_\mu l_L) \\
& - G_S(\bar{s}c)(\bar{\nu}_L l_R) - G_P(\bar{s}\gamma_5 c)(\bar{\nu}_L l_R) \\
& - G_T(\bar{s}\sigma^{\mu\nu} c)(\bar{\nu}_L\sigma_{\mu\nu} l_R) + \text{h.c.}, \tag{21}
\end{aligned}$$

where the terms parameterized by $G_F V_{cs}^*$ represent the effective SM Lagrangian, the other five arose by new type interactions.

A few possibilities can arise the non-Standard contributions to charm meson leptonic and semileptonic decays which have been analyzed in Refs. [24–26, 42, 43]. Other attempts to account for flavour symmetry breaking in pseudoscalar meson decay constants previously presented in Refs. [44–47]. As an example among the candidates which can lead to an effective $\bar{s}c\bar{\nu}l$ vertex they discussed, the mechanism of the u -channel exchange of a charge $-1/3$ scalar leptoquark S_0 is analyzed here. S_0 transforms as color-triplet and weak-singlet with the $U(1)$ hyper-charge $-2/3$ under $SU(3)_c \times SU(2)_L \times U(1)_Y$ transformations of the SM [24, 28]. The interactions between S_0 and the SM fermions can be described as [24]

$$\mathcal{L}_{S_0} = \lambda_{2i}^{LL}(\bar{c}_L l_{iL}^C - \bar{s}_L \nu_{iL}^C)S_0 + \lambda_{2i}^{RR}\bar{c}_R l_{iR}^C S_0 + \text{h.c.}, \tag{22}$$

where the superscript C stands for charge conjugation, the subscript i denotes the generation of lepton, and λ_{2i}^{LL} and λ_{2i}^{RR} are complex Yukawa couplings. When the leptoquark mass satisfy $m_{S_0} \gg m_D$, one can obtain

$$G_V = G_A = \frac{|\lambda_{2i}^{LL}|^2}{4m_{S_0}^2}, \tag{23}$$

$$G_P = G_S = \frac{\lambda_{2i}^{LL}\lambda_{2i}^{RR*}}{4m_{S_0}^2} = -2G_T. \tag{24}$$

Then, there are only two unrelated coefficients left for two type fermion-leptoquark-fermion interactions in Eq. (21). We can name the one parameterized by $|\lambda_{2i}^{LL}|^2/m_{S_0}^2$ the LL type, which is caused by only the scalar leptoquark S_0^L , and the one parameterized by $\lambda_{2i}^{LL}\lambda_{2i}^{RR*}/m_{S_0}^2$ the LR type.

Because of these new interactions, the expression of differential decay rate for $D \rightarrow K\ell\nu_\ell$ decays, Eq. (1), should be rewritten as

$$\begin{aligned}
\frac{d\Gamma_\ell^{NP}}{dq^2} = & \frac{|\mathbf{p}|^3}{24\pi^3} \left(1 - \frac{m_\ell^2}{q^2}\right)^2 \cdot \left\{ \left(1 + \frac{m_\ell^2}{2q^2}\right) \left| \left(G_F V_{cs}^* + \frac{G_V}{\sqrt{2}}\right) f_+^K(q^2) \right|^2 \right. \\
& + \frac{3(m_D^2 - m_K^2)^2}{8m_D^2 |\mathbf{p}|^2} |f_0^K(q^2)|^2 \cdot \left| \frac{m_\ell}{\sqrt{q^2}} \left(G_F V_{cs}^* + \frac{G_V}{\sqrt{2}}\right) + \frac{\sqrt{q^2}G_S}{\sqrt{2}(m_c - m_s)} \right|^2 \\
& + \text{Re} \left[\left(G_F V_{cs}^* + \frac{G_V}{\sqrt{2}}\right) \frac{\mathbf{i} 3\sqrt{2}m_\ell G_T^*}{(m_D + m_K)} f_T^{K*}(q^2) f_+^K(q^2) \right] \\
& \left. + \frac{2\sqrt{2}(q^2 + 2m_\ell^2)}{(m_D + m_K)^2} |G_T f_T^K(q^2)|^2 \right\}, \tag{25}
\end{aligned}$$

where the new form factor, $f_T^K(q^2)$, is defined for describing the contribution of the tensorial operators via [48]

$$\langle K(p_K) | \hat{T}_{\mu\nu} | D(p_D) \rangle = \frac{2(p_K^\mu p_D^\nu - p_K^\nu p_D^\mu)}{m_D + m_K} f_T^K(q^2). \tag{26}$$

where $\widehat{T}_{\mu\nu}$ represents the tensor operator.

To obtain constraints on LL - and LR - type fermion-leptoquark-fermion interactions from $D \rightarrow K\ell\nu_\ell$ decays, we re-analyze the experimental data via Eq. (25) by one type new interaction at a time. The χ^2 (Eq. (11)) is re-construct to be

$$\chi_{NP}^2 = \sum_{i=1}^{98} \sum_{j=1}^{98} (E_i - T_i) (C_{ET}^{-1})_{ij} (E_j - T_j), \quad (27)$$

where E and T are respectively the experimental value and theoretical expectation of $\Delta\Gamma$, \mathbf{f} or f_+^{NL} , C_{ET}^{-1} is the inverse of the covariance matrix C_{ET} , which is a 98×98 matrix. In the context of NP, \mathbf{f}_i^{th} (Eq. (14)) should be rewritten as

$$\mathbf{f}_i^{th} = \frac{\left[\int_{q_{i\min}^2}^{q_{i\max}^2} \frac{d\Gamma_\mu^{NP}/dq^2 \cdot 24\pi^3/|\mathbf{p}|^3/(1 - m_\mu^2/q^2)^2}{G_{FV}^2 [V_\mu + S_\mu (1 + \beta q^2/\alpha)^2]} dq^2 \right]^{\frac{1}{2}}}{f_+^K(0) \sqrt{q_{i\max}^2 - q_{i\min}^2}}, \quad (28)$$

where $G_{FV} = G_F V_{cs}^* + G_V/\sqrt{2}$ and F_i^{th} (Eq. (16)) should be rewritten as

$$F_i^{th} = \left[\frac{\int_{q_{i\min}^2}^{q_{i\max}^2} \left(0.54 \frac{d\Gamma_e^{NP}}{dq^2} + 0.46 \frac{d\Gamma_\mu^{NP}}{dq^2} \right) dq^2}{G_F^2 |\mathbf{p}_i|^3 / 24\pi^3 (q_{i\max}^2 - q_{i\min}^2)} \right]^{\frac{1}{2}}. \quad (29)$$

In our numerical calculations, a complete set of lattice calculations of $f_+^K(q^2)$ and $f_0^K(q^2)$ [37] and $f_T^K(q^2)$ [48] provided by the ETMC and $V_{cs}^* = |V_{cs}| = 0.97351(13)$ (conventionally) obtained from the unitarity constrains [33] are used as SM inputs. The covariance matrix C_{ET} contains the correlations between the experimental measurements and the correlations between the theoretical expectations i.e. $C_{ET} = C_{exp} + C_{th}$. $C_{exp} = C_{\Delta\Gamma} \oplus C_{FOC} \oplus C_{Belle}$ where $C_{\Delta\Gamma}$, C_{FOC} and C_{Belle} can be obtained as the analysis in Section 4.2. C_{th} can be construct via the covariance among the parameters of form factors which are in the ETMC's papers published and the uncertainty of $|V_{cs}|$.

For LL type new interactions, corresponding coefficients are real, the constraints on these coefficients, at 95% C.L., for the case of final states with $e\nu$ pair

$$\frac{|\lambda_{21}^{LL}|^2}{m_{S_0}^2} < 5.4 \times 10^{-6} \text{ (GeV}^{-2}\text{)}, \quad (30)$$

and for the case of final states with $\mu\nu$ pair

$$\frac{|\lambda_{22}^{LL}|^2}{m_{S_0}^2} < 4.0 \times 10^{-6} \text{ (GeV}^{-2}\text{)}. \quad (31)$$

Since the coefficients corresponding to LR type new interactions are complex, the 95% C.L. curves are placed in the real-imaginary plane as shown in Figs.6 (a) for the electron case and (b) for the muon case.

Recently, a search for pair production of second-generation leptoquarks is performed by the CMS Collaboration by using 35.9 fb^{-1} of data collected at $\sqrt{s}=13 \text{ TeV}$ in 2016 with the CMS detector

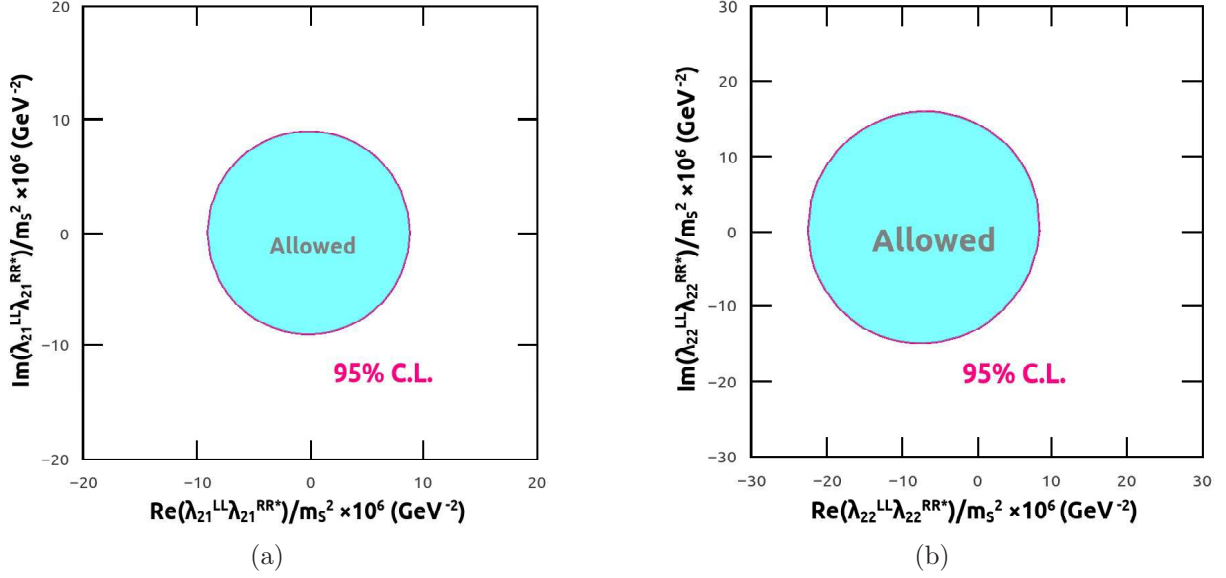


Figure 6: Allowed regions (cyan) of (a) $\lambda_{21}^{LL} \lambda_{21}^{RR*} / m_{S_0}^2$ for the electron case and (b) $\lambda_{22}^{LL} \lambda_{22}^{RR*} / m_{S_0}^2$ for the muon case. The outside of the pink closed curves are excluded at 95% C.L.

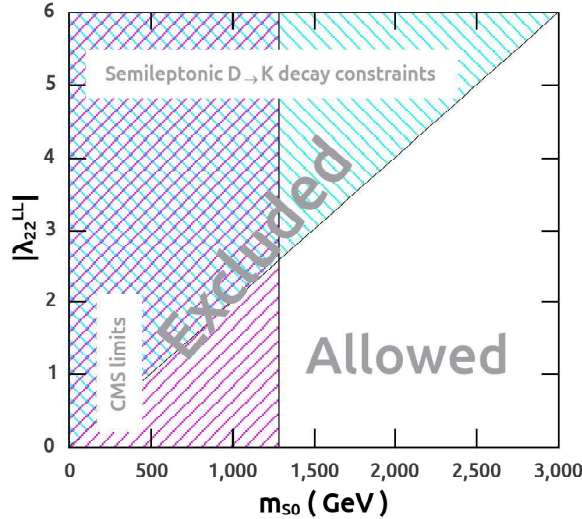


Figure 7: Combined limits on second-generation leptoquark S_0^L .

at the LHC [49]. By analyzing the final states with $\mu\mu jj$ and $\mu\nu jj$, they exclude second-generation leptoquarks with masses less than 1530 GeV (1285 GeV) for $\beta = 1(0.5)$ at 95% C.L., where β is the branching fraction of a leptoquark decaying to a charged lepton and a quark. Assuming lepton number conservation, with limits Eqs. (31) obtained from semileptonic $D \rightarrow K$ decays in conjunction with masses limits for second-generation scalar leptoquarks obtained by the CMS Collaboration, we show the combined limits on second-generation leptoquark S_0^L in Fig. 7.

6 Conclusions

By globally analyzing all existing measurements for $D \rightarrow K\ell^+\nu_\ell$ ($\ell = e, \mu$) decays in the last 30 years, we determined both the vector and scalar form factors of $D \rightarrow K\ell^+\nu_\ell$ decays from these ex-

perimental measurements. With two-parameter series expansion form factors, we obtain the product of form factor $f_+^K(0)$ and the magnitude $|V_{cs}|$ and the shape parameters of both vector and scalar form factors

$$f_+^K(0)|V_{cs}| = 0.7182 \pm 0.0029,$$

$$r_{+1} = -2.16 \pm 0.007, \quad r_{01} = 0.89 \pm 3.27.$$

The shape parameter r_{01} has a quite large uncertainty due to the small contribution of the scalar form factor to the total decay rate, and the precision could be improved if the experimental measurements are done with larger statistical data in future by experiments e.g. BESIII and Belle II.

With the product $f_+^K(0)|V_{cs}|$ together with $|V_{cs}|$ obtained from unitarity constraints, we determine

$$f_+^K(0) = 0.7377 \pm 0.003 \pm 0.000,$$

which is consistent within error with the lattice calculations, and presents a good consistency with the previous fitting result, but with higher precision.

With the product $f_+^K(0)|V_{cs}|$ in conjunction with the average of form factor $f_+^K(0)$ from lattice calculations, the magnitude of CKM matrix element V_{cs} can be extracted

$$|V_{cs}|^{D \rightarrow Kl\nu_l} = 0.964 \pm 0.004 \pm 0.019,$$

where the second error is from the lattice calculated form factor which is 5 times larger than the first error which is from experiments. The determined magnitude $|V_{cs}|$ presents a good consistency within error with the one from SM global fit. Then factoring in $|V_{cs}|^{D_s \rightarrow l\nu_l} = 1.008 \pm 0.021$ determined from leptonic D_s decay [33], the magnitude of the CKM matrix element V_{cs} is determined to be

$$|V_{cs}| = 0.985 \pm 0.014,$$

which is in good agreement within error with the average value $|V_{cs}| = 0.995 \pm 0.016$ from PDG'2016 [33].

We re-analyze these experimental measurements in the context of new physics. Taking the form factors determined from LQCD and $|V_{cs}|$ from unitarity constraints as input parameters, we constrain leptoquark $S_0^{-1/3}$ from $D \rightarrow Kl\nu_l$ at 95% C.L.. The second-generation leptoquark S_0^L and relevant Yukawa couplings are constraint as

$$\frac{|\lambda_{22}^{LL}|^2}{m_{S_0}^2} < 4.0 \times 10^{-6} \text{ (GeV}^{-2}\text{)},$$

Considering recent mass constraints for second-generation leptoquarks obtained by the CMS Collaboration, we give a combined limits on second-generation leptoquark S_0^L .

Acknowledgement

This work was supported in part by the National Natural Science Foundation of China under Grants No.11275088 and 11747318.

References

- [1] C. Liu (2012). arXiv:1207.1171.

- [2] J. C. Anjos *et al.* [Tagged Photon Spectrometer Collaboration], Phys. Rev. Lett. **62** (1989) 1587.
- [3] P. L. Frabetti *et al.* [E687 Collaboration], Phys. Lett. B **315** (1993) 203.
- [4] P. L. Frabetti *et al.* [E687 Collaboration], Phys. Lett. B **364** (1995) 127.
- [5] K. Kodama *et al.* [E653 Collaboration], Phys. Lett. B **336** (1994) 605.
- [6] J. Adler *et al.* [MARK-III Collaboration], Phys. Rev. Lett. **62** (1989) 1821.
- [7] G. D. Crawford *et al.* [CLEO Collaboration], Phys. Rev. D **44** (1991) 3394.
- [8] J. M. Link *et al.* [FOCUS Collaboration], Phys. Lett. B **598** (2004) 33.
- [9] A. Bean *et al.* [CLEO Collaboration], Phys. Lett. B **317** (1993) 647.
- [10] B. Aubert *et al.* [BaBar Collaboration], Phys. Rev. D **76** (2007) 052005.
- [11] M. Ablikim *et al.* [BES Collaboration], Phys. Lett. B **597** (2004) 39.
- [12] M. Ablikim *et al.* [BES Collaboration], Phys. Lett. B **608** (2005) 24.
- [13] M. Ablikim *et al.* [BES Collaboration], hep-ex/0610019.
- [14] M. Ablikim *et al.* [BES Collaboration], Phys. Lett. B **644** (2007) 20.
- [15] D. Besson *et al.* [CLEO Collaboration], Phys. Rev. D **80** (2009) 032005.
- [16] M. Ablikim *et al.* [BESIII Collaboration], Phys. Rev. D **92** (2015) no.7, 072012.
- [17] M. Ablikim *et al.* [BESIII Collaboration], Chin. Phys. C **40** (2016) no.11, 113001.
- [18] M. Ablikim *et al.* [BESIII Collaboration], Eur. Phys. J. C **76** (2016) no.7, 369.
- [19] M. Ablikim *et al.* [BESIII Collaboration], Phys. Rev. D **96** (2017) no.1, 012002.
- [20] J. M. Link *et al.* [FOCUS Collaboration], Phys. Lett. B **607** (2005) 233.
- [21] J L. Widhalm *et al.* [Belle Collaboration], Phys. Rev. Lett. **97** (2006) 061804.
- [22] Y. Fang, G. Rong, H. L. Ma and J. Y. Zhao, Eur. Phys. J. C **75** (2015) no.1, 10.
- [23] <http://pdg.lbl.gov/2017/reviews/rpp2017-rev-ckm-matrix.pdf>
- [24] A. S. Kronfeld, PoS LATTICE **2008** (2008) 282.
- [25] B. A. Dobrescu and A. S. Kronfeld, Phys. Rev. Lett. **100** (2008) 241802.
- [26] J. Barranco, D. Delepine, V. Gonzalez Macias and L. Lopez-Lozano, J. Phys. G **43** (2016) no.11, 115004.
- [27] W. Buchmuller, R. Ruckl and D. Wyler, Phys. Lett. B **191** (1987) 442 Erratum: [Phys. Lett. B **448** (1999) 320].
- [28] I. Doršner, S. Fajfer, A. Greljo, J. F. Kamenik and N. Košnik, Phys. Rept. **641** (2016) 1.
- [29] F. Su and Y. D. Yang, Int. J. Mod. Phys. A **26** (2011) 3185.

- [30] D. Becirevic and A. B. Kaidalov, Phys. Lett. B **478** (2000) 417.
- [31] D. Scora and N. Isgur, Phys. Rev. D **52** (1995) 2783.
- [32] T. Becher and R. J. Hill, Phys. Lett. B **633** (2006) 61.
- [33] C. Patrignani *et al.* [Particle Data Group], Chin. Phys. C **40** (2016) no.10, 100001.
- [34] Y. Amhis *et al.* [HFLAV Collaboration], Eur. Phys. J. C **77** (2017) no.12, 895.
- [35] S. Dobbs *et al.* [CLEO Collaboration], Phys. Rev. D **77** (2008) 112005.
- [36] T. Kaneko *et al.* (JLQCD Collaboration), EPJ Web Conf. **175** (2018) 13007.
- [37] V. Lubicz *et al.* (ETM Collaboration), Phys. Rev. D **96** (2017) no.5, 054514.
- [38] S. Aoki *et al.*, Eur. Phys. J. C **77** (2017) no.2, 112.
- [39] A. Khodjamirian, C. Klein, T. Mannel and N. Offen, Phys. Rev. D **80** (2009) 114005.
- [40] H. Y. Cheng and X. W. Kang, Eur. Phys. J. C **77** (2017) no.9, 587 Erratum: [Eur. Phys. J. C **77** (2017) no.12, 863]
- [41] L. Riggio, G. Salerno and S. Simula, arXiv:1706.03657.
- [42] I. Dorsner, S. Fajfer, J. F. Kamenik and N. Kosnik, Phys. Lett. B **682** (2009) 67.
- [43] S. Fajfer, I. Nisandzic and U. Rojcek, Phys. Rev. D **91** (2015) no.9, 094009.
- [44] S. S. Gershtein and M. Y. Khlopov, Pisma Zh. Eksp. Teor. Fiz. **23** (1976) 374.
- [45] M. Y. Khlopov, Sov. J. Nucl. Phys. **28** (1978) 583 [Yad. Fiz. **28** (1978) 1134].
- [46] Y. Y. Komachenko and M. Y. Khlopov, Yad. Fiz. **45** (1987) 467 [Sov. J. Nucl. Phys. **45** (1987) 295].
- [47] Y. Y. Komachenko and M. Y. Khlopov, Sov. J. Nucl. Phys. **46** (1987) 679 [Yad. Fiz. **46** (1987) 1164].
- [48] V. Lubicz, L. Riggio, G. Salerno, S. Simula and C. Tarantino, arXiv:1803.04807 [hep-lat].
- [49] CMS Collaboration (CMS Collaboration), CMS-PAS-EXO-17-003.